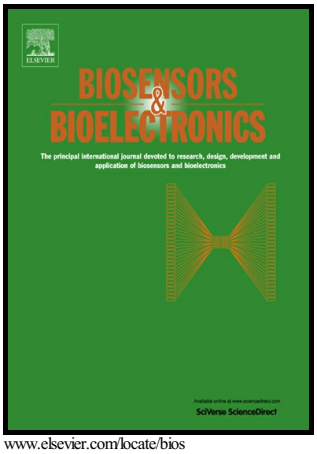

www.elsevier.com/locate/bios

An electrochemical biosensor to simultaneously detect VEGF and PSA for early prostate cancer diagnosis based on graphene oxide/ssDNA/PLLA nanoparticles

Lung-Hsuan Pan, Shin-Hung Kuo, Tzu-Yang Lin, Chih-Wen Lin, Po-Yu Fang, Hung-Wei Yang

PII: S0956-5663(16)30092-6
DOI: http://dx.doi.org/10.1016/j.bios.2016.01.077
Reference: BIOS8417

To appear in: *Biosensors and Bioelectronic*

Received date: 27 November 2015
Revised date: 28 December 2015
Accepted date: 28 January 2016

Cite this article as: Lung-Hsuan Pan, Shin-Hung Kuo, Tzu-Yang Lin, Chih-Wer Lin, Po-Yu Fang and Hung-Wei Yang, An electrochemical biosensor to simultaneously detect VEGF and PSA for early prostate cancer diagnosis base on graphene oxide/ssDNA/PLLA nanoparticles, *Biosensors and Bioelectronic* http://dx.doi.org/10.1016/j.bios.2016.01.077

An electrochemical biosensor to simultaneously detect VEGF and PSA for early prostate cancer diagnosis based on graphene oxide/ssDNA/PLLA nanoparticles

Lung-Hsuan Pan [a], Shin-Hung Kuo [b], Tzu-Yang Lin [a], Chih-Wen Lin [c], Po-Yu Fang [d], Hung-Wei Yang [a,*]

[a] Institute of Medical Science and Technology, National Sun Yat-sen University, Kaohsiung 80424, Taiwan

[b] Department of Electrical Engineering, National Cheng Kung University, Tainan 70101, Taiwan

[c] Department of Chemical Engineering, National Tsing Hua University, Hsinchu 30013, Taiwan

[d] School of Chemistry and Biochemistry, Georgia Institute of Technology, Atlanta, GA, 30332, USA.

* Corresponding author:

Tel.: +886-7-5252000x5842; Fax: +886-7-5250151

E-mail address: howardyang@mail.nsysu.edu.tw

Abstract

Early diagnosis of prostate cancer (PCa) is critical for the prevention of metastasis and for early treatment; therefore, a simple and accurate device must be developed for this purpose. In this study, we reported a novel fabrication method for producing a dual-modality biosensor that can simultaneously detect vascular endothelial growth factor (VEGF) and prostate-specific antigen (PSA) in human serum for early diagnosis of PCa. This biosensor was constructed by coating graphene oxide/ssDNA (GO-ssDNA) on an Au-electrode for VEGF detection, and incorporated with poly-$_L$-lactide nanoparticles (PLLA NPs) for signal amplification and PSA detection. The results showed that this biosensor has wide liner detection ranges (0.05-100 ng/mL for VEGF and 1-100 ng/mL for PSA), as well as high levels of sensitivity and selectivity (i.e., resisting interference from external factors, such as glucose, ascorbic acid human serum protein, immunoglobulin G, and immunoglobulin M), and demonstrated a high correlation with an enzyme-linked immunosorbent assay for sample detection in patients. Therefore, this biosensor could be utilized for early clinical diagnosis of PCa in the future.

Keywords: graphene oxide, single strand DNA, vascular endothelial growth factor (VEGF), prostate-specific antigen (PSA), electrochemical biosensor, prostate cancer (PCa)

1. Introduction

Graphene is an elite of carbon nanomaterials because of its unique chemical and physical properties, such as large surface area, strong mechanical strength, optical properties, biocompatibility, and excellent thermal and electrical conductivity (Shao et al., 2010). Compared with graphite and glassy carbon, graphene exhibits low

charge-transfer resistance and broad electrochemical potential (Zhou et al., 2009). Graphene associated with its planar structure also shows an excellent electron transfer effectiveness as a suitable material for electrochemical biosensors compared with other types of carbon nanomaterials (Tang et al., 2009). In addition to electrochemical potential, the unique electro-optical properties of graphene enhance the mid-infrared signal to produce a high-sensitivity optical biosensor for detection of protein molecules (Rodrigo et al., 2015). Graphene based biosensors create various prospects for diagnosis in the future. The first report on mechanical exfoliation of monolayer graphene was published in 2004 (Novoselov et al., 2004) showing graphene to be the most powerful two-dimensional nanomaterial for use in numerous applications (Chen et al., 2015). Graphene based biosensors are widely used to detect glucose, cholesterol, dopamine, immunoglobulin G (IgG), Immunoglobulin E (IgE), uric acid (UA), ascorbic acid (AA), DNA, proteins, cells, and small biochemicals (Vashist et al., 2015). Therefore, graphene based biosensors are considered a promising system for early cancer diagnosis.

PCa occurs when a malignant tumor is induced by the mutation of DNA. It is the most commonly lethal type of cancer among men aged 50 to 80 years old (Oesterling et al., 1993). Because PCa in its early stage is difficult to detect, mortality rates increase each year (Schröder et al., 2009). Clinical diagnosis methods are ultrasonography, digital rectal inspection, computed tomography scan, magnetic resonance imaging, and cancer protein assay (Catalona et al., 1994; Catalona et al., 1997; Mitchell et al., 2008). Prostate-specific antigen (PSA) is the most effective serum marker available for the clinical detection of PCa, and clinical data show that serum values higher than 4.0 ng/mL are abnormal (Ushaa et al., 2011). Moreover, some patients may receive a false positive diagnosis for PCa because of prostatic hyperplasia, prostatitis, benign prostate hyperplasia, or cystitis, which can all increase

PSA levels (Stephan et al., 2007). Vascular endothelial growth factor (VEGF) is another critical cancer biomarker that is overexpressed in numerous types of human cancers, including brain tumors, lung cancer, breast cancer, urinary tract tumors, and gastrointestinal cancer. It is also active in angiogenesis, vasculogenesis, and endothelial cell growth, thereby causing endothelial cell proliferation, promoting cell migration, inhibiting apoptosis, and inducing blood vessel permeabilization (Lin et al., 2015; Kwon et al., 2010; Roskoski, 2007). A higher VEGF intratumoral protein level is present in tissue with cervical cancer than in normal cervical tissue. In addition, a higher level of VEGF leads to an increased risk of lymph node metastasis under these conditions. Therefore, VEGF may be a suitable candidate as a biomarker for enhancing the accuracy of PCa diagnosis with PSA.

Several systems for detecting VEGF and PSA have been developed, and are primarily based on using an enzyme-linked immunosorbent assay (ELISA), fluorescence, electrochemical technologies (Sarkar et al., 2002; Mohammad et al., 2013), surface plasmon resonance, and surface-enhanced Raman scattering (Cho et al., 2012; Zhao et al., 2011; Li et al., 2007). Because of various types of procedures, the detection of VEGF and PSA is prone to error, relatively time consuming, and expensive. Therefore, we demonstrated the effective capture and rapid electrochemical detection of VEGF and PSA simultaneously in serum samples from a patient with PCa by using a graphene oxide/ssDNA (GO-ssDNA) based biosensor incorporated with dual-antibody modified PLLA NPs to amplify the electrochemical signal. This is the first study that focuses on the combined analysis of VEGF and PSA by using only one label-free biosensor with human blood samples for the diagnosis of PCa. This dual examination approach potentially offers a more accurate and rapid alternative than current tests do, and is based on immunological methods, such as an ELISA and immunohistochemistry.

2. Materials and methods

2.1. Chemicals

Graphite platelets (model xGnP; width 100 μm, thickness 5-15 nm) were obtained from XG Sciences Inc. (East Lansing, MI, USA). Acrylic acid, potassium persulfate, sulfuric acid (H_2SO_4, 98%), sodium sulfate (Na_2SO_4), potassium permanganate ($KMnO_4$), hydrogen peroxide solution (H_2O_2), and ammonia were purchased from Showa Chemical Co. (Tokyo, Japan). Human $VEGF_{165}$ was purchased from PeproTech Inc. (Rocky Hill, NJ, USA). Branched polyethylenimine (bPEI), 1-Ethyl-3-(3-dimethylaminepropyl) carbodiimide hydrochloride (EDC.HCl), *N*-hydroxysulfosuccinimide sodium salt (sulfo-NHS), 2-(*N*-morpholino) ethanesulfonic acid hydrate (MES), sulfosuccinimidyl 4-(*N*-maleimidomethyl)cyclohexane-1-carboxylate (sulfo-SMCC), glucose, AA, UA, IgG, and immunoglobulin M (IgM) were purchased from Sigma-Aldrich (St. Louis, MO, USA). Fetal bovine serum (FBS) was purchased from Biological Industries (Kibbutz Beit Haemek, Israel). The anti-VEGF antibody ($VEGF_{ab}$), anti-PSA antibody (PSA_{ab}), VEGF ELISA assay kit (Human VEGF Immunoassay), and PSA ELISA assay kit (Human PSA Immunoassay) were purchased from Abcam (Cambridge, MA, USA). Deionized (DI) water was used in all experiments. DNA oligonucleotide for recognizing VEGF was synthesized and purified by Sigma-Aldrich (St. Louis, MO, USA). The sequence of the employed oligomers was as follows:

ssDNA: 5'-SH-$(CH_2)_6$-TGT GGG GGT GGA CGG GCC GGG TAGA-3'.

2.2. Preparation of bPEI modified GO

A carboxylated GO (GO-COOH) sheet modified with 1-one-butyric acid was prepared as previously described (Stankovich et al., 2006; Stankovich et al., 2007). The bPEI was immobilized on the GO as follows. EDC (24 mg) and sulfo-NHS (27 mg) were dissolved in the dark in 2 mL of MES. A 0.1-mL aliquot of this solution was mixed with 0.1 mL of GO-COOH (5 mg/mL) at 25°C, and this mixture was sonicated in the dark for 30 min. After separation, the activated GO-COOH was washed with 0.8 mL of MES and resuspended in 0.1 mL of MES; it was then mixed with 0.1 mL of bPEI solution (2%) at 25°C for 3 h. Materials with bPEI immobilized on the GO-COOH surface (GO-bPEI) were separated out of the solution, washed with PBS to remove any unimmobilized bPEI, and dispersed in 0.2 mL of PBS.

2.3. Preparation of GO-ssDNA

The ssDNA was immobilized on the GO-bPEI by using a two-step reaction scheme. First, the GO-bPEI was mixed with excess sulfo-SMCC at 25°C and incubated in the dark for 60 min. After being separated and washed with DI water, the sulfo-SMCC-conjugated GO-bPEI was mixed with thiol-mediated ssDNA at 5°C and vortexed in the dark for 12 h. The ssDNA was immobilized on the surface of the GO-bPEI to form GO-ssDNA, which was separated from the solution and washed with DI water. The binding capacity of ssDNA immobilized on GO-bPEI was calculated using a spectrophotometer (SpectraMax M2, Molecular Devices, USA) at 260 nm to measure the concentration of unbound ssDNA in the supernatant and in the washing solution.

2.4. Preparation of dual-antibody modified PLLA nanoparticles

The carboxylated poly-$_L$-lactide (PLLA–COOH) (2 g) in methylene chloride (10 mL) was converted to PLLA–NHS with excess EDC and NHS in a MES buffer (0.5 M, pH 6.3) at 25°C for 2 h. PLLA–NHS was precipitated with ethyl ether (5 mL), and repeatedly washed in an ice-cold mixture of ethyl ether and methanol to remove residual NHS. After drying under a vacuum, PLLA–NHS (1 g) was dissolved in chloroform (4 mL), followed by the addition of Poly(ethylene glycol) 2-aminoethyl ether acetic acid (NH_2–PEG–COOH, 250 mg) and N,N-diisopropylethylamine (28 mg). After reacting for 12 h, the co-polymer was precipitated with cold methanol and washed three times with the same solvent (5 mL each time) to remove unreacted NH_2–PEG–COOH. The resulting PLLA–PEG–COOH block co-polymer was dried under a vacuum.

The PLLA–PEG–COOH polymer solution (10 mg/mL) was prepared in dimethylformamide (DMF). Nanoparticles (NPs) were formed by adding the polymer solution to water (the ratio of solvent to water can be 1:5 or 1:10) in a sonication washing machine. The resulting NP suspension was stirred while uncovered for 6 h at room temperature and then purified using centrifugation (10 min, 10,000 rpm). PLGA-PEG-COOH NPs were reacted with a mixture of EDC and sulfo-NHS solution at 25°C and vortexed in the dark for 40 min. After separation, NPs were washed three times with 0.8 mL of 0.1 M MES buffer resuspended in 0.2 mL of 0.1 M MES, and then mixed with 0.1 mL of $VEGF_{ab}$ solution and 0.1 mL of PSA_{ab} solution at 5°C in the dark for 12 h. The solution was then washed with DI water and dispersed in 0.2 mL of DI water to form dual-antibody modified PLLA NPs.

2.5. Fabrication of the Au-electrode based biosensor

The Au-electrode used for VEGF and PSA detection was fabricated using the Micro-Electro-Mechanical Systems (MEMS) techniques. The electrochemical module consists of three-electrode modules, which include an Au working electrode, an Au counter electrode, and a commercial Ag/AgCl reference electrode. To simplify the experimental procedure, we constructed an Au-based two electrode system containing working and counter electrodes simultaneously on a glass substrate. The fabrication processes involved three steps: metal-film deposition, photolithography, and metal etching. The glass substrate (80 × 80 × 1.1 mm, Beautiful Rich Photoelectric Material Co., Ltd., Taiwan) was first cleaned using piranha (the volume ratio H_2SO_4 to H_2O_2 was 3:1) at 120°C for 10 min. After ultrasonic cleaning in acetone for 5 min, the glass substrate was then rinsed with isopropyl alcohol and DI water.

To fabricate the Au electrode layers from the MEMS process, metal-film was deposited on the glass substrate. Chromium (Cr) with a thickness of 15 nm was first deposited onto the glass substrate as an adhesion layer, and a 200 nm-thick piece of gold (Au) was then deposited using an E-beam evaporator (F.S.E Co., Taiwan). After metal-film deposition, a photolithography process was used to define Au electrode patterns. An AZ1500 photoresist with a thickness of 1.5 μm was span onto the glass substrate in two steps: 500 rpm for 10 s and 3000 rpm for 30 s. The photoresist was soft baked at 90°C for 90 s and then patterned using Mask Aligner (Suss MicroTec MA 150CC, NDL, Taiwan). Exposure time was 12 s (12 mW/cm^2, I-line) and development time was approximately 90 s using an AD-10 developer. The pattern on the Au layer was created using a metal etching process. The metal etching time was 30 s for a 200-nm Au layer of Au etchant and 10 s for a Cr layer of Cr etchant. Thus, both types of Au electrodes (i.e., working and counter electrodes) were fabricated.

The fabrication process was completed by washing the electrodes with acetone, isopropyl alcohol, and DI water (Figure S1). In addition, plastic tape was used to separate the electrode into a sensing area and an electrical area.

The working area on the electrode was coated with 10 μL of GO-ssDNA solution and dried overnight at 25°C in the hood to form the GO-ssDNA based biosensor for detection of VEGF and PSA.

2.6. Determination of VEGF concentrations using an ELISA assay

We used a human VEGF ELISA kit (ab100663) and human PSA ELISA kit (ab188388), and followed the manufacturer's protocols to determine VEGF and PSA concentrations in human serum samples.

2.7. Preparation of serum samples for quantitative detection

The human plasma samples were prepared as follows. Plasma was collected from a whole blood sample (10 mL) treated with heparin anticoagulant and centrifuged at 3,500 rpm and at 4°C for 15 min. The supernatant (serum) was collected for VEGF detection. This study was approved by the Institutional Review Board of the Chang Gung Memorial Hospital, Taiwan (IRB: 104-7457A3).

2.8. VEGF and PSA detection on the GO-ssDNA based biosensor

The process of electrochemical detection by the GO-ssDNA based biosensor in 1 mM ($K_3[Fe(CN)_6]$)/($K_4[Fe(CN)_6]$) and 0.1 M KCl solution was used to establish the baseline current before any samples were measured. For the VEGF standard curve, the GO-ssDNA based biosensor was soaked into 500 μL of various concentrations of VEGF solution incubated for 30 min. The biosensor was washed three times with DI water and soaked into the dual-antibody modified PLLA NPs solution for 30 min then

using differential pulse voltammetry (DPV) to measure the current response. After measurement, the GO-ssDNA-PLLA based biosensor was soaked into 500 μL of various concentrations of PSA solution and incubated for 30 min to measure PSA concentration (Scheme 1A).

All measurements were obtained using a 0.05-V bias voltage. The change in current (ΔC) that resulted from VEGF or PSA binding to the GO-ssDNA based biosensor was calculated as follows: $\triangle I = Ii - Ic$ (Ii = the mean baseline current of the GO-ssDNA based biosensor; Ic = the mean current of the GO-ssDNA based biosensor after incubation with VEGF or PSA at any concentration).

3. Results and discussion

3.1. Characterizations of the GO-ssDNA-PLLA based biosensor

The scheme of the prepared GO-ssDNA nanosheets is shown in Scheme 1B. To enhance the solubility and conjugating rate of GO-COOH, the surface of GO-COOH was first modified with bPEI to form amine-terminated GO (GO-bPEI) with numerous amine functional groups on the surface. It confirmed by the zeta potential that was changed to +56.5 mV (GO-bPEI) from -46.3 mV (GO-COOH). The 5'-thiol-modified ssDNA was then conjugated onto GO-bPEI by using sulfo-SMCC linkers. X-ray photoelectron spectroscopy (XPS) proved that bPEI and ssDNA were conjugated on the GO-COOH. The GO-COOH sample showed C1s and O1s peaks at 284 eV and 532 eV, respectively. After bPEI and ssDNA conjugation, a peak at 399 eV (N1s) for GO-bPEI and a peak at 198 eV (P2s) for GO-ssDNA appeared, indicating that the bPEI was conjugated on the GO-COOH and that the ssDNA was conjugated on the GO-bPEI (Figure 1A).

The Au-electrode system used to prepare the VEGF and PSA sensors in this work was fabricated using the MEMS techniques. The schematic diagram designed

for the fabrication of the Au-electrode prototype is shown in Figure 1B. The diameter of the sensing area was 3.8 mm and the width of the counter electrode was 1.0 mm. The entire size of the sensor area was 14 × 40 mm^2, and the actual sensing area was 11.34 mm^2 on the working electrode. Atomic force microscopy (AFM) was used to analyze the thickness and roughness (Ra) on the electrode after layer-by-layer deposition (Figure 1C). The images showed that the thickness and Ra were increased after each modification step. After VEGF deposition, the thickness and Ra were increased to 15–25 nm and 2.2 nm, respectively, compared with GO-ssDNA. The thickness and Ra were further increased to 60–100 nm and 6.65 nm, respectively, while the dual-antibody modified PLLA NPs (average diameter of 76 nm was measured using Nano Particle Analyzed (SZ-100, HORIBA, Japan)) bound to the VEGF on the electrode, indicating that the layer-by-layer deposition on the electrode was successful that could be used for further PSA detection.

3.2. Stability and reusability of the Au-electrode

Electrodes are typically produced using plastic and metal elements that may cause environmental damage; thus, reusable electrodes would be more environmentally friendly. To determine if electrodes can be reused, we reused the same Au-electrode to reconstruct the GO-ssDNA biosensor and repeated the electrochemical measurement. The deposited materials on the working area of the Au-electrode were washed away after measurement, and the biosensor was reconstructed by depositing the GO-ssDNA on the working area. The results showed that our presented Au-electrode could be reused approximately 24 times without significant current change (<5%) compared with the commercial Au-electrode (up to 5 times) because Cr with a thickness of 15 nm was initially deposited onto the glass substrate before Au deposition to enhance adhesion to the presented Au-electrode.

The results confirmed the reusability of our Au-electrode and the stable covering process of the GO-ssDNA solution. The relative responses indicated an excellent relative standard deviation (RSD) of 4.53% (Figure 2A). We also investigated the parting of Au-thin film on the working area after various time periods of reconstruction and electrochemical measurement. The Au-thin film of the commercial Au-electrode started to peel off at the 2nd-time of reconstruction and the Au-electrode was completely damaged at the 6th-time of reconstruction. However, the Au-electrode used in this study maintained the completeness of the Au-thin film until the 24th-time of reconstruction (Figure S2).

3.3. Electrochemical characterization of the GO-ssDNA modified Au-electrode

The electrochemical behavior of the GO-ssDNA modified Au-electrode was studied using cyclic voltammetry (CV) and DPV in a 1 mM ($K_3[Fe(CN)_6]$)/($K_4[Fe(CN)_6]$), and was a best redox indicator for providing a convenient and valuable approach for analyzing the electron transfer between the solution and the electrode surface, which occurred by tunneling through either the barrier of the interfaces or through defects in the barrier (Prabhulkar et al., 2009). We activated the Au-electrode in 0.1 M KCl solution until two obvious peaks appeared at 0.55 V and 0.78 V before we began the CV study. The CV results showed nearly complete reversible behavior on the bare Au-electrode, the GO-ssDNA modified Au-electrode, the GO-ssDNA-VEGF-PLLA biosensor, and the GO-ssDNA-VEGF-PLLA-PSA biosensor from -0.2–0.6 V at a scan rate of 40 mV/s (Figure S3). The current was significantly decreased to 24.4 μA from 64.4 μA after deposition of GO-ssDNA on the Au-electrode, which blocked the electron transfer, indicating that the GO-ssDNA was uniformly coated on the working area surface. In this study, we designed dual-antibody modified PLLA NPs (with $VEGF_{ab}$ and PSA_{ab}

modification on the surface) for electrochemical signal amplification and PSA detection, which resulted in the current decreasing to 18.7 μA from 24.4 μA (10 ng/mL of VEGF only) and to 16.6 μA from 18.7 μA (dual-antibody modified PLLA NPs). The current was further decreased to 13.6 μA after the addition of 10 ng/mL of PSA, indicating that the VEGF and PSA could be effectively captured and detected using the same biosensor. The signal change can be attributed to the effects of steric blockage and charge repulsion/attraction effects (de la Escosura-Muñiz et al., 2013; Rodriguez et al., 2005).

3.4. Interference and performance of the GO-ssDNA based biosensor

During the interference study, we incubated a GO-ssDNA biosensor with typical interfering species that exists in human plasma, including IgG (1000 ng/dL), IgM (192.5 μg/dL), glucose (5 mM), AA (4.3 μg/mL), UA (0.295 mM) (Khan et al., 2011; Marquette et al., 2003), 10% FBS, and human serum protein (1 mg/mL). The results were evaluated on the basis of the ΔC with the addition of different species in the GO-ssDNA biosensor (Figure S4). Additional washing with DI water was performed after hybridization, and prior to measurement, to eliminate the influence of other interfering species. No significant current changes were detected with the addition of the typical types of interfering species (0.023-0.393 μA). Furthermore, a significant ΔC (21.28 μA) was observed after the addition of VEGF (100 ng/mL) in the presence of the interfering species, which was also observed for treatment with the same concentration of only VEGF (20.92 μA), indicating that this GO-ssDNA based biosensor resisted interference well and had excellent selectivity.

In this study, the dual-antibody modified PLLA NPs were designed to amplify the current signal for VEGF detection and for PSA detection. Therefore, we had to ensure that the $VEGF_{ab}$ and PSA_{ab} were conjugated on the surface of PLLA NPs. The

dual-antibody modified PLLA NPs were stained using TRITC-labeled secondary antibody (for PSA_{ab}) and FITC-labeled secondary antibody (for $VEGF_{ab}$), and dropped on the glasses (Figure 2B). The results showed that the dual-antibody modified PLLA NPs exhibited strong red and green fluorescence compared with the naked PLLA NPs, indicating that the $VEGF_{ab}$ and PSA_{ab} were conjugated on the surface of the PLLA NPs.

To further investigate the optimization of the GO-ssDNA based biosensor, DPV was used to measure the ΔC generated by ferricyanide ($[Fe(CN)_6]^{3-/4-}$) at 0.24 V. Before the capture of VEGF, the sensor displayed a peak current of 99.1 μA at 0.24 V, corresponding to the redox reaction between $[Fe(CN)_6]^{3-/4-}$ and the sensor surface. This current decreased with increasing VEGF concentration (with the same trend for PSA) because of the depletion of charge carriers in the Au-electrode when more negatively charged PLLA NPs bound to the VEGF-functionalized surface. The ΔC increased linearly with increasing VEGF concentrations from 50 pg/mL to 100 ng/mL, the detection range was wider than that concentrations were observed without the incorporation of PLLA NPs (125 pg/mL to 100 ng/mL) (Figures 3A and B). The ΔC also increased linearly with increasing PSA concentrations from 1 ng/mL to 100 ng/mL (Figures 3C and D). No lower concentration of PSA could be detected because the thickness of the detection layer was significantly greater than the Debye length after PLLA NP modification, which would have reduced the electric field effect (Li et al., 2012). However, this biosensor still can be used for effective PSA detection because the concentration of PSA in patients with PCa would be significantly higher than 4 ng/mL. These results indicated that this biosensor could accurately detect VEGF and PSA simultaneously.

3.5. Determination of VEGF and PSA in human plasma

VEGF is a critical biomarker for cancer growth and is often over-expressed in tumors (Kido et al., 2001). Furthermore, patients with various types of tumors (including PCa) typically express higher concentrations of VEGF in their serum than healthy individuals do (Kaya et al. 2004; Poon et al. 2003). In addition, the concentrations of PSA higher than 4.0 ng/mL are considered abnormal. Therefore, the combination of VEGF and PSA detection would be helpful for accurate early diagnosis of PCa. In this study, the accuracy of the GO-ssDNA based biosensor in detecting VEGF and PSA was confirmed for determining its applicability in clinical diagnoses. The serum samples were collected from patients diagnosed with early stages of PCa to assess the utility of our GO-ssDNA based biosensor; these results were also compared with those results obtained from a conventional detection method (i.e., an ELISA). The VEGF and PSA concentrations were calculated using the calibration curves of electrochemical sensing and an ELISA. The GO-ssDNA based biosensor detected the concentrations of VEGF in the serum of three patients, which were 180.2, 198.7, and 183.6 pg/mL, respectively; and the concentrations of PSA in the same serum samples were 11.3, 11.9, and 13.2 ng/mL, respectively (Figure 4). In this study, the obtained raw data were compared with the ELISA results; we observed no significant difference in the VEGF and PSA levels detected using the two methods, which indicated that this dual examination approach potentially offers a more accurate and rapid alternative (within 60 min for detection of two biomarkers) than current tests that are based on immunological methods, such as an ELISA and immunohistochemistry.

4. Conclusion

In this study, we presented a new method of fabrication for GO-ssDNA based biosensors by simultaneously using dual-antibody modified PLLA NPs for signal amplification, VEGF, and PSA detection. A glass chip with an Au-electrode was modified with GO-ssDNA and used for the capture and detection of VEGF; the dual-antibody modified PLLA NPs were added to recognize the VEGF for signal amplification. The dual-antibody modified PLLA NPs on the biosensor could be further used to capture and detect PSA. The detection limits for the VEGF and PSA were 50 pg/mL and 1 ng/mL, respectively, and this was achieved within a period of 60 min. In addition, this biosensor detected VEGF and PSA in the human serum of patients with PCa at concentrations similar to those detected with an ELISA. This is the first label-free electrochemical system that can be used to rapidly and accurately detect two types of cancer biomarkers. We anticipate that this biosensor may be a promising platform for point-of-care medical diagnostics, and could rival other commercially available instruments in the future.

Acknowledgements

We thank the Ministry of Science and Technology of the Republic of China, Chang Gung Memorial Hospital, and the Food Industry Research and Development Institute for the financial assistance provided (MOST103-2320-B-110-004-MY2, CMRPG3E2041, CMRPG3B1601, GERPD2E0031). We would also like to thank the Chang Gung Memorial Hospital Microscopy Core Laboratory and National Nano Device Laboratories for their assistance.

References

Catalona, W.J., Richie, J.P., Ahmann, F.R., Hudson, M.A., Scardino, P.T., Flanigan, R.C., deKernion, J.B., Ratliff, T.L., Kavoussi, L.R., Dalkin, B.L., et al., 1994. J. Urol. 151, 1283-1290.

Catalona, W.J., Smith, D.S., Ornstein, D.K., 1997. JAMA 277, 1452-1455.

Chen, Y., Tan, C., Zhang, H., Wang, L., 2015. Chem. Soc. Rev. 44, 2681-2701.

Cho, H., Yeh, E.C., Sinha, R., Laurence, T.A., Bearinger, J.P., Lee, L.P., 2012. ACS Nano 6, 7607-7614.

de la Escosura-Muñiz, A., Chunglok, W., Surareungchai, W., Merkoçi, A., 2013. Biosens. Bioelectron. 40, 24–31.

Kaya, A., Çiledag, A., Gulbay, B.E., Poyraz, B.M., Çelik, G., Sen, E., Savas, H., Savas, I., 2004. Respir. Med. 98, 632–636.

Kido, S., Kitadai, Y., Hattori, N., Haruma, K., Kido, T., Ohta, M., Tanaka, S., Yoshihara, M., Sumii, K., Ohmoto, Y., Chayama, K., 2001. Eur. J. Cancer 37, 1482–1487.

Kwon, O.S., Park, S.J., Jang, J., 2010. Biomaterials 31, 4740–4747.

Li, X., Zhang, J., Gu, H., 2012. Langmuir 28, 2827-2834.

Li, Y., Hye, J.L., Corn, R.M., 2007. Anal. Chem. 79, 1082-1088.

Lin, C.W., Wei, K.C., Liao, S.S., Huang, C.Y., Sun, C.L., Wu, P.J., Lu, Y.J., Yang, H.W., Ma, C.C.M., 2015. Biosens. Bioelectron. 67, 431-437.

Mitchell, P.S., Parkin, R.K., Kroh, E.M., Fritz, B.R., Wyman, S.K., Pogosova-Agadjanyan, E.L., Peterson, A., Noteboom, J., O'Briant, K.C., Allen, A., Lin, D.W., Urban, N., Drescher, C.W., Knudsen, B.S., Stirewalt, D.L., Gentleman, R., Vessella, R.L., Nelson, P.S., Martin, D.B., Tewari, M., 2008. P. Natl. Acad. Sci. USA 105, 10513-10518.

Mohammad, J.K., Ahmadi, M.T., Elnaz, A., Meisam, R., Hediyeh, K., Che Harun, F.K., 2013. J. Biosens. Bioelectron. 4, 1000131.

Novoselov, K.S., Geim, A.K., Morozov, S.V., Jiang, D., Zhang, Y., Dubonos, S.V., Grigorieva, I.V., Firsov, A.A., 2004. Science 306, 666-669.

Oesterling, J.E., Jacobsen, S.J., Chute, C.G., Guess, H.A., Girman, C.J., Panser, L.A., Lieber, M.M., 1993. JAMA 270, 860-864.

Poon, R.T.P., Lau, C.P.Y., Cheung, S.T., Yu, W.C., Fan, S.T., 2003. Cancer Res. 63, 3121–3126.

Prabhulkar, S., Alwarappan, S., Liu, G., Li, C.Z., 2009. Biosens. Bioelectron. 24, 3524–3530.

Rodrigo, D., Limaj, O., Janner, D., Etezadi, D., García de Abajo, F.J., Pruneri, V., Altug, H., 2015. Science 349, 165-168.

Rodriguez, M.C., Kawde, A.N., Wang, J., 2005. Chem. Commun. 34, 4267–4269.

Roskoski, R.J., 2007. Crit. Rev. Oncol. Hemat. 62, 179-213.

Sarkar, P., Pal, P.S., Ghosh, D., Setford, S.J., Tothill, I.E., 2002. Int. J. Pharm. 238, 1-9.

Schröder, F.H., Hugosson, J., Roobol, M.J., Tammela, T.L.J., Ciatto, S., Nelen, V., Kwiatkowski, M., Lujan, M., Lilja, H., Zappa, M., Denis, L.J., Recker, F., Berenguer, A., Määttänen, L., Bangma, C.H., Aus, G., Villers, A., Rebillard, X., van der Kwast, T., Blijenberg, B.G., Moss, S.M., de Koning, H.J., Auvinen, A., 2009. New Engl. J. Med. 360, 1320-1328.

Shao, Y., Wang, J., Wu, H., Liu, J., Aksay, I.A., Lin, Y., 2010. Electroanalysis 22, 1027-1036.

Stankovich, S., Dikin, D.A., Dommett, G.H.B., Kohlhaas, K.M., Zimney, E.J., Stach, E.A., Piner, R.D., Nguyen, S.T., Ruoff, R.S., 2006. Nature 442, 282–286.

Stankovich, S., Dikin, D.A., Piner, R.D., Kohlhaas, K.A., Kleinhammes, A., Jia, Y., Wu, Y., Nguyen, S.T., Ruoff, R.S., 2007. Carbon 45, 1558–1565.

Stephan, C., Cammann, H., Meyer, H.A., Lein, M., Jung, K., 2007. Cancer Lett. 249, 18-29.

Tang, L., Wang, Y., Li, Y., Feng, H., Lu, J., Li, J., 2009. Adv. Funct. Mater. 19, 2782-2789.

Ushaa, S.M., Madhavilatha, M., Rao, G.M., 2011. Int. J. Nano Biomater. 3, 239-255.

Vashist, S.K., Luong, J.H.T., 2015. Carbon 84, 519-550.

Zhao, S., Yang, W., Lai, R.Y., 2011. Biosens. Bioelectron. 26, 2442-2447.

Zhou, M., Zhai, Y., Dong, S., 2009. Anal. Chem. 81, 5603-5613.

Figure legends:

Scheme 1. (A) Scheme of electrochemical detection of VEGF and PSA in samples using the GO-ssDNA based biosensor. (B) Scheme of the procedure for preparation of GO-ssDNA. (B) XPS surface survey spectra of GO-COOH, GO-bPEI, and GO-ssDNA. (C) The schematic diagram designed for the Au-electrodes.

Figure 1. (A) XPS surface survey spectra of GO-COOH, GO-bPEI, and GO-ssDNA. (B) The schematic diagram designed for the Au-electrodes. (C) AFM images of GO-COOH, GO-bPEI, GO-ssDNA, GO-ssDNA-VEGF, and GO-ssDNA-VEGF-PLLA NPs (top) and their curves of thickness distribution (bottom).

Figure 2. (A) Reusability and stability of our Au-electrode and a commercial Au-electrode. Our electrode showed no decrease in function after 24 times of reconstruction (RSD = 4.53%). (B) Phase contrast (top) and fluorescence images (middle and bottom) of PLLA NPs and dual-antibody modified PLLA NPs. (Red color: staining with TRITC-labeled secondary antibody; green color: staining with FITC-labeled secondary antibody).

Figure 3. (A) DPV showing the decrease in the electrochemical signal upon incubation of the electrode in samples with various concentrations of VEGF and the fixed concentration of dual-antibody modified PLLA NPs. (B) Calibration curve for the ΔC according to the results of DPV at various VEGF concentrations (n = 6). (C) DPV showing the decrease in the electrochemical signal upon incubation of the electrode in samples with various concentrations of PSA. (D) Calibration curve for the ΔC according to the results of DPV at various PSA concentrations (n = 6).

Figure 4. (A) Plasma VEGF concentrations measured using the GO-ssDNA based biosensor and an ELISA (n = 3). (B) Plasma PSA concentrations measured using the GO-ssDNA based biosensor and an ELISA (n = 3). (Note: the VEGF and PSA concentrations were detected using the same sample).

Highlights

- Novel GO-ssDNA based biosensor incorporated with dual-antibody modified PLLA NPs was prepared.
- Simultaneous detection of VEGF and PSA in same one electrochemical biosensor.
- Achieving wide linear range of detection of 0.05~100 ng/mL (VEGF) and 1~100 ng/mL (PSA).
- Highly sensitive and selective detection of VEGF and PSA was achieved in human serum.

Figure(s)

Scheme 1

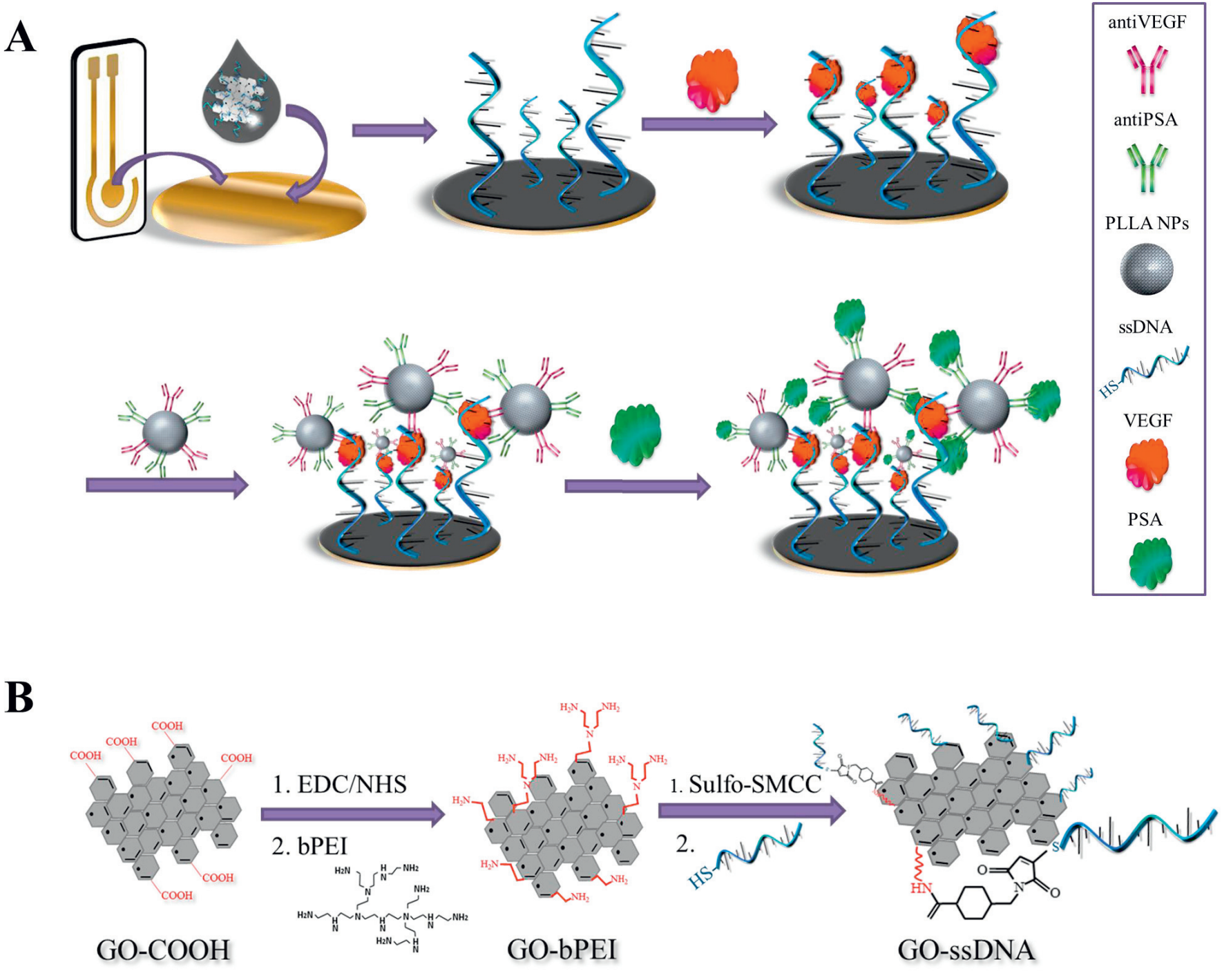

Figure 1

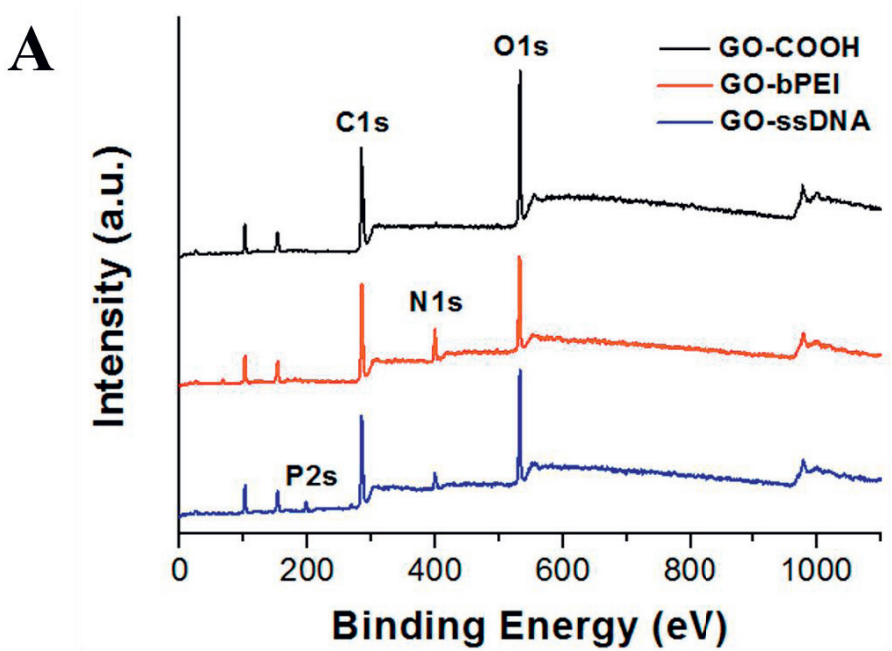
A
GO-COOH
GO-bPEI
GO-ssDNA
O1s
C1s
N1s
P2s
Intensity (a.u.)
0
200
400
600
800
1000
Binding Energy (eV)

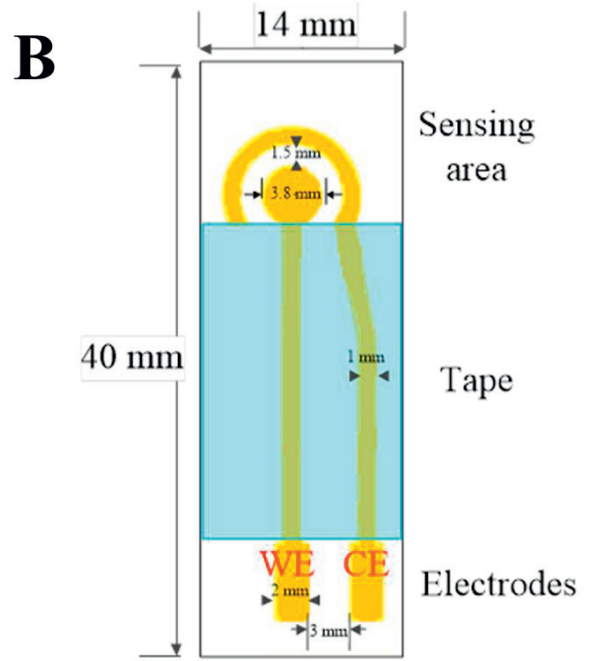
B
14 mm
40 mm
Sensing area
1.5 mm
3.8 mm
1 mm
Tape
WE
CE
2 mm
3 mm
Electrodes

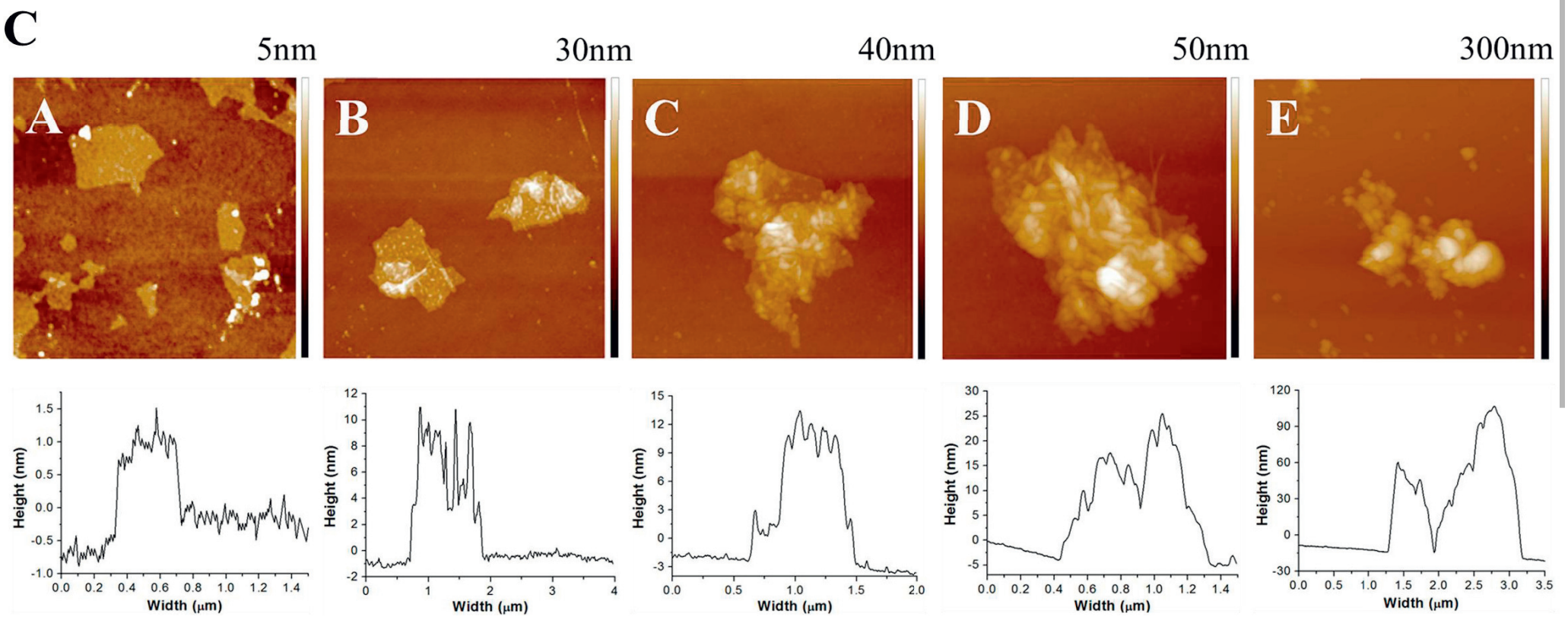
C
5nm
30nm
40nm
50nm
300nm
A
B
C
D
E
Height (nm)
Width (μm)

Figure 2

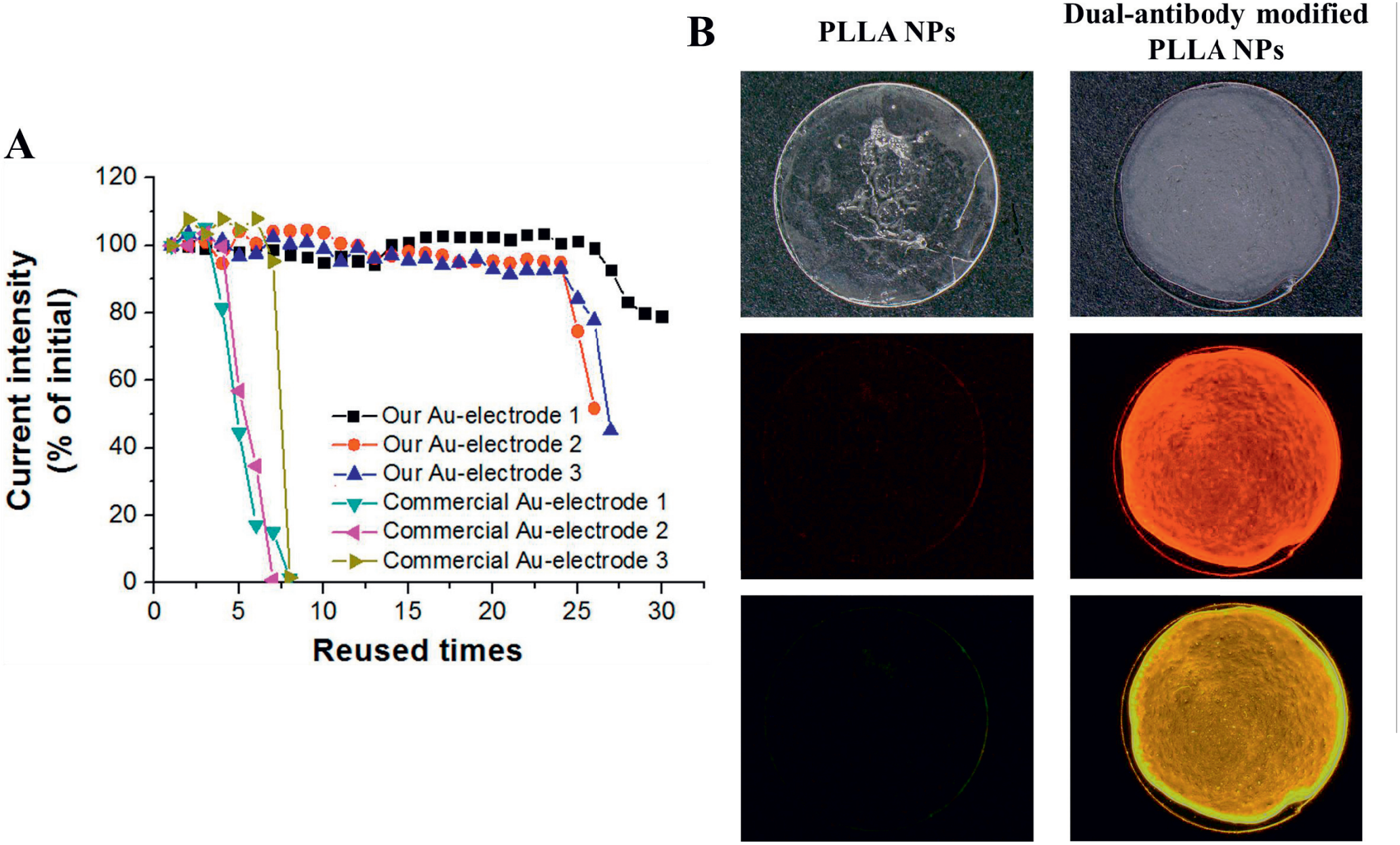
A
Current intensity
(% of initial)
120
100
80
60
40
20
0
0
5
10
15
20
25
30
Reused times
Our Au-electrode 1
Our Au-electrode 2
Our Au-electrode 3
Commercial Au-electrode 1
Commercial Au-electrode 2
Commercial Au-electrode 3
B
PLLA NPs
Dual-antibody modified
PLLA NPs

Figure 3

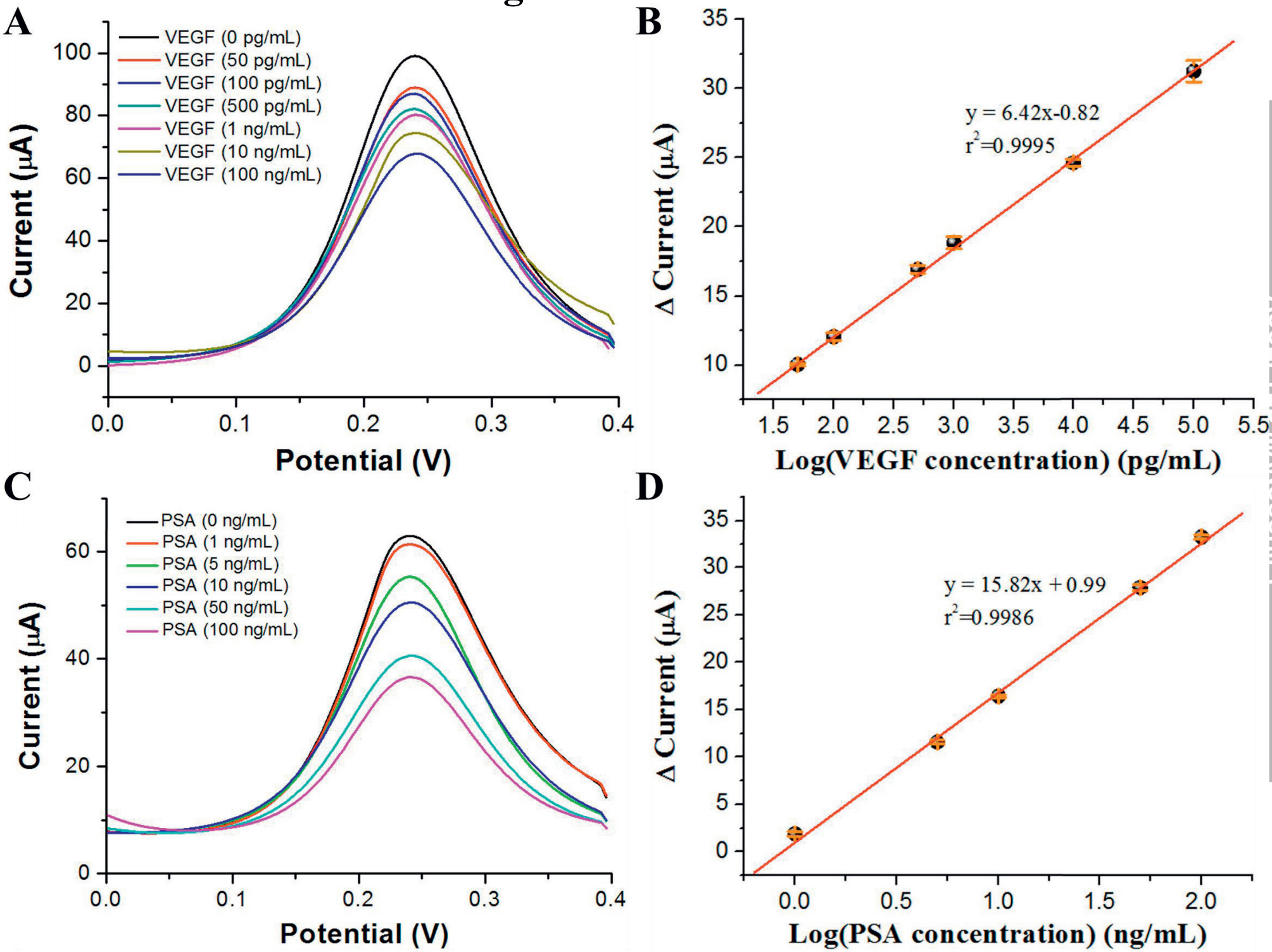

Figure 4